REPORT DOCUMENTATION PAGE

Form Approved
OMB No. 0704-0188

1. REPORT DATE *(DD-MM-YYYY)*	**2. REPORT TYPE**	**3. DATES COVERED** *(From - To)*
January 2013	Technical Paper	January 2013-May 2013

4. TITLE AND SUBTITLE
Enhanced Cyanate Ester Nanocomposites through Improved Nanoparticle Surface Interactions

5a. CONTRACT NUMBER
In-House

5b. GRANT NUMBER

5c. PROGRAM ELEMENT NUMBER

6. AUTHOR(S)
Christopher Sahagun, Andrew Guenthner, Joseph Mabry

5d. PROJECT NUMBER

5e. TASK NUMBER

5f. WORK UNIT NUMBER
Q0BG

7. PERFORMING ORGANIZATION NAME(S) AND ADDRESS(ES)

Air Force Research Laboratory (AFMC)
AFRL/RQRP
10 E. Saturn Blvd.
Edwards AFB CA 93524-7680

8. PERFORMING ORGANIZATION REPORT NO.

9. SPONSORING / MONITORING AGENCY NAME(S) AND ADDRESS(ES)
Air Force Research Laboratory (AFMC)
AFRL/RQR
5 Pollux Drive
Edwards AFB CA 93524-7048

10. SPONSOR/MONITOR'S ACRONYM(S)

11. SPONSOR/MONITOR'S REPORT NUMBER(S)
AFRL-RQ-ED-TP-2013-012

12. DISTRIBUTION / AVAILABILITY STATEMENT
Distribution A: Approved for Public Release; Distribution Unlimited. PA#13119

13. SUPPLEMENTARY NOTES
Conference paper for the 2013 International SAMPE Meeting, Long Beach, CA, 6-9 May 2013.

14. ABSTRACT
This work presents the results of an investigation into the role of silica nanoparticle surface chemistry in the enhancement of cyanate ester nanocomposite properties. Previous work has shown that the incorporation of silica nanoparticles improves the thermo-oxidative qualities, moisture uptake properties and processability of cyanate ester resins. This work seeks to better understand the root of these improvements by comparing thermal and mechanical properties as a function of nanoparticle loading and surface treatment using both polar and non-polar as well as potentially reactive surface functionalities. This presentation will focus on the structure-process-property relationships of various silica nanoparticle/cyanate ester systems with a discussion of the implications for novel composite processing techniques.

15. SUBJECT TERMS

16. SECURITY CLASSIFICATION OF:			**17. LIMITATION OF ABSTRACT**	**18. NUMBER OF PAGES**	**19a. NAME OF RESPONSIBLE PERSON**
					Joseph Mabry
a. REPORT	**b. ABSTRACT**	**c. THIS PAGE**			**19b. TELEPHONE NO** *(include area code)*
Unclassified	**Unclassified**	**Unclassified**	SAR	13	661-525-5857

Standard Form 298 (Rev. 8-98)
Prescribed by ANSI Std. 239.18

ENHANCED CYANATE ESTER NANOCOMPOSITES THROUGH IMPROVED NANOPARTICLE SURFACE INTERACTIONS

Christopher M. Sahagun[1], Andrew J. Guenthner[2], Joseph M. Mabry[2]
[1]National Research Council / Air Force Research Laboratory
[2]Air Force Research Laboratory, Aerospace Systems Directorate
10 E. Saturn Blvd.
Edwards AFB, CA 93524

ABSTRACT

This work presents the results of an investigation into the role of silica nanoparticle surface chemistry in the enhancement of cyanate ester nanocomposite properties. Previous work has shown that the incorporation of silica nanoparticles improves the thermo-oxidative qualities, moisture uptake properties and processability of cyanate ester resins. This work seeks to better understand the root of these improvements by comparing thermal and mechanical properties as a function of nanoparticle loading and surface treatment using both polar and non-polar as well as potentially reactive surface functionalities. This presentation will focus on the structure-process-property relationships of various silica nanoparticle/cyanate ester systems with a discussion of the implications for novel composite processing techniques.

1. INTRODUCTION

The favorable thermal, physical and processing characteristics of cyanate ester resins make them an ideal choice for the matrix material of high-temperature reinforced polymer composites. As with other composite matrices, the physical properties of cyanate ester resins can be modified by the incorporation of nanoscale silica particles into the thermoset molecular network. This type of property modification is very effective as only a few weight percent of silica nanoparticles are required to induce observable changes in a polymeric matrix [1]. For example, the addition of a few weight percent silica has been shown to reduce water uptake in a crosslinked epoxy coating [2], increase stiffness and toughness in a DGEBA-based epoxy system [3], improve the dynamic mechanical properties and thermal stability while reducing water uptake in a polyimide film [4] and, for the case of thermoplastic polyethylene, the addition of silica nanoparticles was found to increase the dielectric breakdown strength and voltage endurance [5]. The improvement in properties is generally thought to originate in the interfacial region between the polymeric matrix and the silica nanoparticle [1, 5, 6, 7]. This small region has a role in property enhancement that is disproportionate to its size in the overall volume of the nanocomposite material. It is reasonable, therefore, to anticipate that tuning the interaction between the nanoparticle surface and the polymer matrix may be an effective means to further improve the physical properties of a polymer nanocomposite material.

A few investigations into the physical properties and cure behavior of cyanate ester/silica nanoparticles have been reported. Fumed silica nanoparticles have been shown to increase the storage modulus of a Bisphenol-E based cyanate ester resin [8]. Additionally, silica particles have been found to improve thermal stability and thermal conductivity of cyanate ester resins intended for electronic applications [9]. Fumed silica nanoparticles have been found to display a

catalytic effect on the polymerization kinetics of a Bisphenol-E based cyanate ester resin [10]. This catalytic effect has been ascribed to hydroxyl groups found at the surface of the particle and also adventitious water adsorbed onto the surface of the particle. Regardless, this catalytic effect is not always desired, especially for the fabrication of large parts where a rapid evolution of heat during the cure reaction may lead to uncontrolled exotherm of the resin. Replacing or sterically blocking these surface hydroxyl groups through the chemical functionalization of the nanoparticle surface is a facile means of eliminating this catalytic behavior of the fumed silica nanoparticles. In addition to reducing catalysis, modification of the silica nanoparticle surface provides an opportunity to explore the potential improvement of physical properties by tuning the interfacial interaction of the silica nanoparticles with the cyanate ester matrix.

This study is an investigation of the influence of nanoparticle surface chemistry on cure behavior and in the enhancement of the physical properties of a cyanate ester/silica nanoparticle system. Three types of surfaces were chosen for investigation; a hydrophilic hydroxyl surface, a hydrophobic octyl surface and a chemically active 3-aminopropyl surface. The cure behavior and thermal properties of the cyanate ester/modified silica nanocomposites were measured with respect to both differences in nanoparticle surface chemistry and loading level.

2. EXPERIMENTATION

2.1 Cyanate Ester Resin

The dicyanate ester of Bisphenol E (LECy) was purchased from Lonza and was used as received. The cyanate ester groups of the LECy monomer undergo a trimerization reaction upon heating to produce a triazine ring that serves as the crosslinking point. Figure 1 shows the chemical structure of the LECy monomer (left) and the triazine ring formed during the cure reaction. No catalyst was used in the cure reaction.

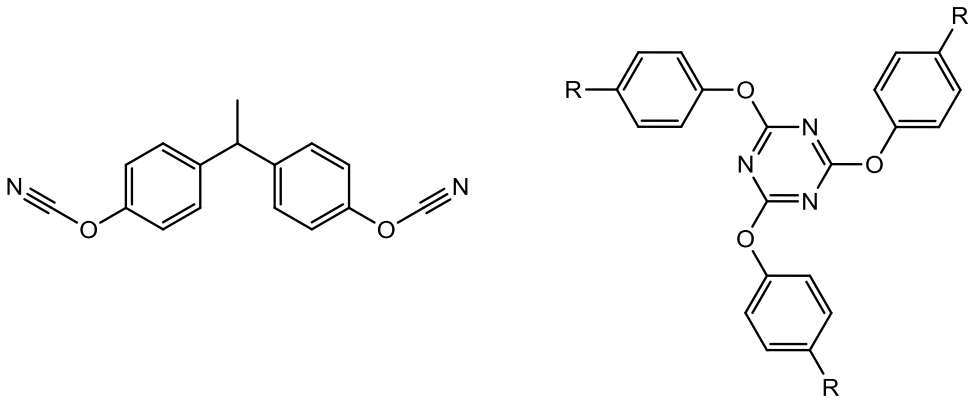

LECy Monomer Triazine Crosslinking Point

Figure 1. Chemical structures of LECy monomer and triazine ring formed during the network building reaction.

2.2 Silica Nanoparticle Filler

Aerosil 200 and Aerosil R805, a hydrophilic fumed silica with hydroxyl surface moieties and a fumed silica with an octyl-modified hydrophobic surface, respectively, were purchased from Degussa. Aerosil 200 particles have a nominal specific surface area of 200 m^2/g while Aerosil R805 particles have a nominal specific surface area of 150 m^2/g. Nanoparticles with a chemically active 3-aminopropyl surface were prepared by treating Aerosil 200 particles with 3-aminopropyltrimethoxy silane. Ten grams of Aerosil 200 were placed in a large round bottomed flask. The flask was affixed to a Schlenk line and dried at 200 °C for 24 hours under vacuum. The sample was then cooled to room temperature and the flask was backfilled with nitrogen. A large excess of 3-aminopropyltrimethoxy silane was dissolved in 500 mL of dry chloroform and added to the round bottomed flask. Care was taken to avoid the introduction of ambient moisture into the reaction flask. The mixture was then allowed to stir for nine days at room temperature under nitrogen. The particles were then removed and any residual unreacted 3-aminopropytrimethoxy silane and side products were removed by three days of Soxhlet extraction in a cellulose thimble with chloroform as the extraction medium.

2.3 Nanocomposite Fabrication

Samples with six different loading levels were prepared for each type of nanoparticle surface. The nanocomposites were prepared in such a way as to yield samples with identical total nanoparticle surface area per gram of LECy (see Table 1 for details). This was necessary as Aerosil 200 and Aerosil R805 have different specific surface areas. Samples with the same loading by mass would not have the same amount of overall nanoparticle/matrix interfacial area, thereby complicating the comparison of the influence of the nanoparticle surface on the final properties of the nanocomposite. Loading levels of each sample are given in Table 1.

Nanocomposite samples were prepared by adding the appropriate amount of silica nanoparticles and LECy to a 20 mL scintillation vial. The vial was lightly shaken by hand to coarsely disperse the silica nanoparticles in the uncured resin. The scintillation vial was then placed in a sonicator with a water bath heated to 50 °C. The sonicator was set to de-gas for 5 minutes and then to sonicate for 60 minutes. This method produced samples that visually appeared to be homogeneously dispersed. There was no noticeable difference between samples with different surface modifications.

After sonication, the LECy/silica nanoparticle mixture was poured into a silicone mold approximately 3 mm deep and 5 mm in diameter. The filled molds were placed in a programmable oven capable of maintaining an inert nitrogen atmosphere. Aerosil 200/LECy nanocomposite samples were cured by ramping from 100 °C to 150 °C at 1 °C per minute, holding for four hours and then ramping to 175 °C at 0.5 °C per minute and holding for 10 hours. This cure schedule, however, was visibly observed to severely undercure the nanocomposites with octyl and 3-aminopropyl surface moieties, providing a good initial indication that the nanoparticle surface has some influence on the cure behavior. After following the cure schedule used for hydroxyl surface nanocomposites these samples then were ramped to 210 °C at 0.5 °C per minute and held at this temperature for 6 hours. After curing, the samples were cut in half with a high speed diamond saw with one half being set aside for testing and the other half

postcured at 290 °C for one hour to drive the reaction to near full conversion. This technique produced small semicircular samples with a light amber color with some haziness observed in samples with high loading levels. The postcured samples were noticeably darker than non-postcured samples.

Table 1. Silica nanoparticle loading levels for the samples used in this study.

Nanoparticle Surface Area Per Gram of LECy (m^2)	Mass of Silica Nanoparticles Per Gram of LECy (g)		
	Hydroxyl Surface	Octyl Surface	3-aminopropyl Surface
1	0.005	0.007	0.005
2	0.010	0.013	0.010
3	0.015	0.020	0.015
4	0.020	0.026	0.020
6	0.030	0.040	0.030
8	0.040	0.056	0.040

2.4 Characterization Techniques

All DSC measurements were conducted with a TA Instruments Q2000 differential scanning calorimeter. Three to five milligrams of sample were placed in an aluminum pan and hermitically sealed. The heat of reaction for each sample was determined by monitoring the heat flow as the samples were ramped from 50 °C to 360 °C at 10 °C per minute. The baseline needed for analysis was obtained by then re-ramping the cured material according to the same protocol. The overall heat of reaction was obtained by integrating the area of the exotherm peak above the baseline scan. The reaction onset temperature was determined by identifying the temperature at which the results of the baseline scan first deviated from the results of the cure scan. All data analysis was performed with Microsoft Excel.

TGA measurements were obtained with a TA Instruments Q5000 Thermogravimetric Analyzer to assess the stability of the surface modification at curing temperatures. Approximately 8 mg of each nanoparticle was ramped from 175 °C to 290 °C at 2.5 °C/min and held for one hour. All data analysis was performed with Microsoft Excel.

FT-IR measurements were made to verify the chemical modification of the nanoparticle surface. Modified nanoparticles were mixed with KBr at 1% loading by weight. The mixture was pressed into pellets and a Nicolet 6700 from Thermo Electron Corporation was used to obtain absorbance spectra. Sixty four scans were made of each sample with a resolution of 4 cm^{-1}. All data analysis was performed with Microsoft Excel.

Thermomechanical measurements were made with a Q400 TMA from TA Instruments. All measurements were made with an applied force of 0.20 N modulated by 0.10 N at 0.05 Hz. A rapid temperature ramp was used in order to reduce the occurrence of in situ cure during the measurement. The sample was ramped from 50 °C to 390 °C at 50 °C/min while monitoring the storage and loss moduli. The thermal lag of the sample was then immediately determined by

repeatedly cycling the temperature chamber from -50 °C to 150 °C at 50 °C/min while monitoring the difference in the temperature lag between the heating and cooling cycles. It was determined that the temperature of the sample lagged the measured temperature by around 30 °C for each sample. Once thermal lag had been established the sample was again ramped to 390 °C at 50 °C per minute in order to determine the "fully cured" T_g. The glass transition temperature was taken to be the point at which the loss modulus reached a peak value. All data analysis was performed with Microsoft Excel.

AFM images were obtained to examine nanoparticle dispersion at the nanoscale. Topographic AFM images were obtained with a Dimension 3100 AFM from Digital Instruments. All imaging was done in tapping mode with a typical etched silicon tip operated at its resonance frequency. Image analysis was performed with Gwyddion SPM analysis software.

3. RESULTS

3.1 Chemical Modification of the Silica Nanoparticle Surface

Figure 2 shows FT-IR spectra of each modified silica nanoparticle. The spectra are dominated by the absorption that is due to the silica core (seen below around 1450 cm^{-1}). Evidence for the chemical modification of the silica surface is found in the broad –OH adsorption band from 3000 cm^{-1} to around 3600 cm^{-1}. This band is the strongest for the unmodified hydroxyl surface (Aerosil 200) and weaker for each of the two modified surfaces. The reduced absorbance in this region after treatment results from surface hydroxyl groups being replaced by the surface modifying agent. The octyl modified surface shows absorption due to -CH stretch at around 2900 cm^{-1}.

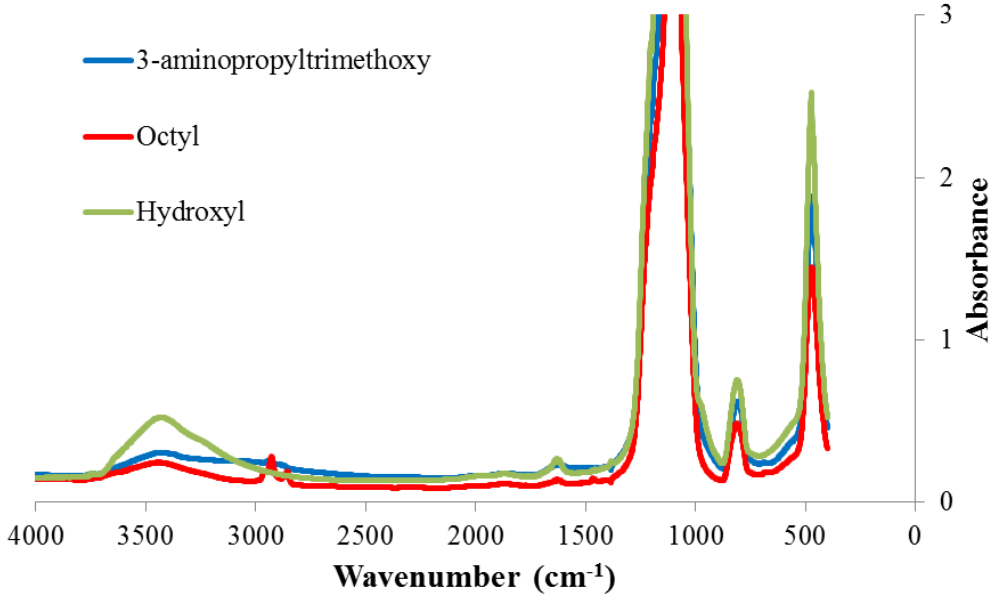

Figure 2. FT-IR spectra of neat modified silica nanoparticles showing chemical modification of the nanoparticle surface.

Figure 3 shows isothermal TGA measurements of the modified silica nanoparticles at temperatures similar to those encountered during the processing of the nanocomposite samples. Little mass loss is observed demonstrating that the chemical modification is stable throughout the processing temperature range used in this study.

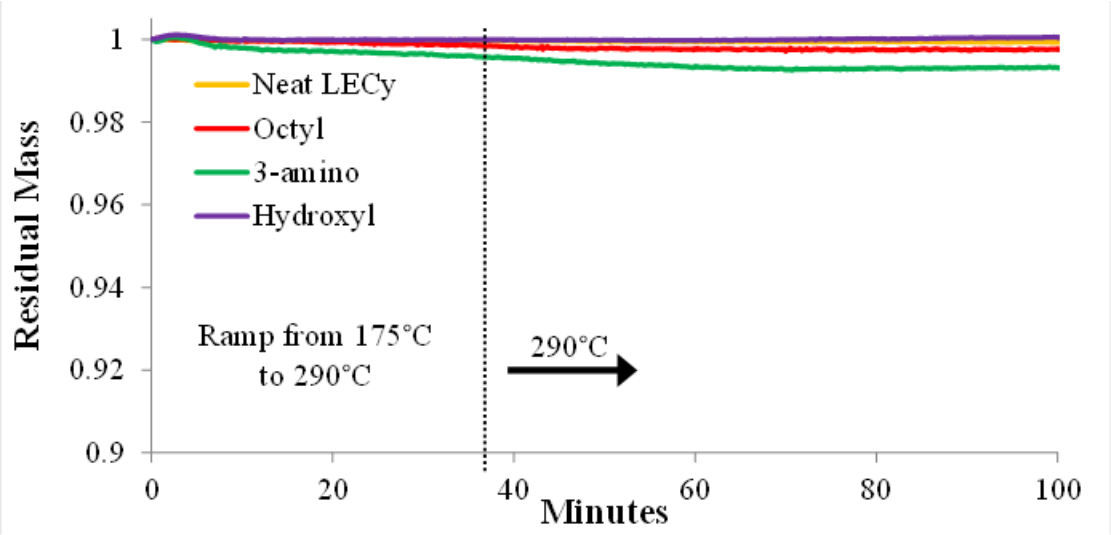

Figure 3. Isothermal TGA of silica nanoparticles showing no significant degradation at processing temperatures.

3.2 Silica Nanoparticle Dispersion

Figure 4 shows topographic AFM images of the fracture surface of neat LECy as well as each of the three nanocomposites. These images show samples with the highest loading of silica nanoparticles (8 m^2 of surface area per gram of LECy). The neat LECy sample shows the relatively flat surface that would be expected of fracture propagation through an elastic homogeneous material. The other images, however, show varying amounts of agglomeration of the silica nanoparticles. Better dispersion of the nanoparticles is indicated by smaller, less frequent agglomeration while the opposite is true for poor dispersion. The fracture surface of the 3-aminopropyl modified silica nanoparticles shows less agglomeration than either the hydroxyl or octyl surfaces and therefore shows better dispersion. The growing cyanate ester network is neither wholly hydrophilic nor wholly hydrophobic. The 3-aminopropyl modified surface has a similar hydrophilic/hydrophobic character as the matrix which likely makes it more compatible with the uncured cyanate ester monomer during mixing. Additionally, the amine of the 3-aminopropyl moiety is chemically active with the cyanate group of the cyanate ester monomer. It is possible that the amine reacts with the cyanate group early in the reaction, effectively functionalizing the silica nanoparticle with a cyanate ester group and thereby increasing the compatibility of the silica nanoparticle with the growing thermoset matrix during the cure reaction.

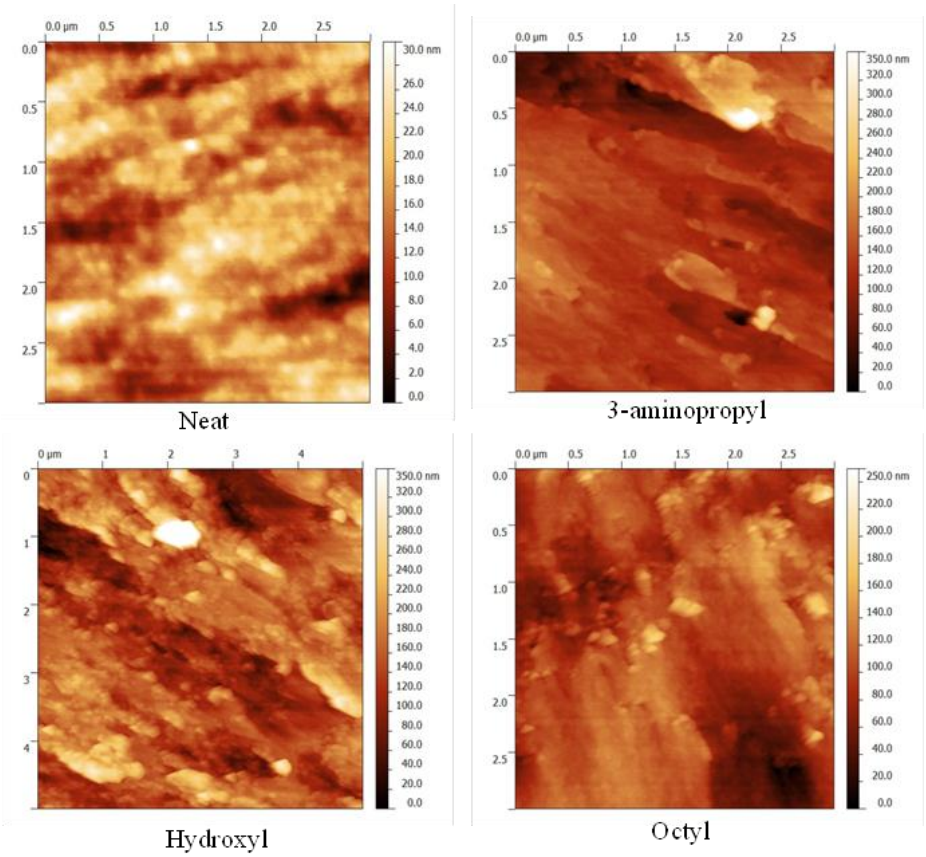

Figure 4. Topographic AFM images of sample fracture surfaces. Neat LECy shows a smooth surface (note the scale bar) while all nanocomposite samples show some degree of nanoparticle agglomeration.

3.3 The Influence of Surface Modification on Chemical Kinetics

Figure 5 shows the integrated heats of reaction for each modified silica nanoparticle as a function of loading level. The integrated heat of reaction is the sum of all heat evolved during the cure reaction. Any nanoparticle-induced change in the reaction products or signification changes to the reaction pathway will cause a change in the overall amount of heat evolved during cure. Figure 5 shows similar overall heats of reaction for all surface types at all loading levels. This indicates that the silica nanoparticles do not strongly influence either the final network structure of the thermoset matrix or the reaction pathway of the curing reaction.

Figure 6 shows the reaction onset temperature of each sample at different loading levels. The reaction onset temperature was taken to be the temperature at which the DSC first detects heat evolution from the curing reaction during a temperature scan of the sample. A reduction in the reaction onset temperature indicates catalytic action within the sample. Figure 6 reveals this type of catalytic effect in samples containing nanoparticles with a hydroxyl surface. Alcohols such as phenols have been shown to have such a catalytic effect on the curing reaction of cyanate ester resins [11]. Neither the octyl functionalized nor the 3-aminopropyl functionalized surfaces show this effect. This result shows that a combination of eliminating some surface hydroxyl groups

and sterically blocking residual hydroxyl groups is a means of reducing the catalytic influence of the nanoparticle surface. This result is important for the fabrication of larger nanocomposite parts where catalytic action may cause an uncontrolled exotherm. For this case, functionalized nanoparticles may be used as the particulate filler to reduce or eliminate the catalytic effect.

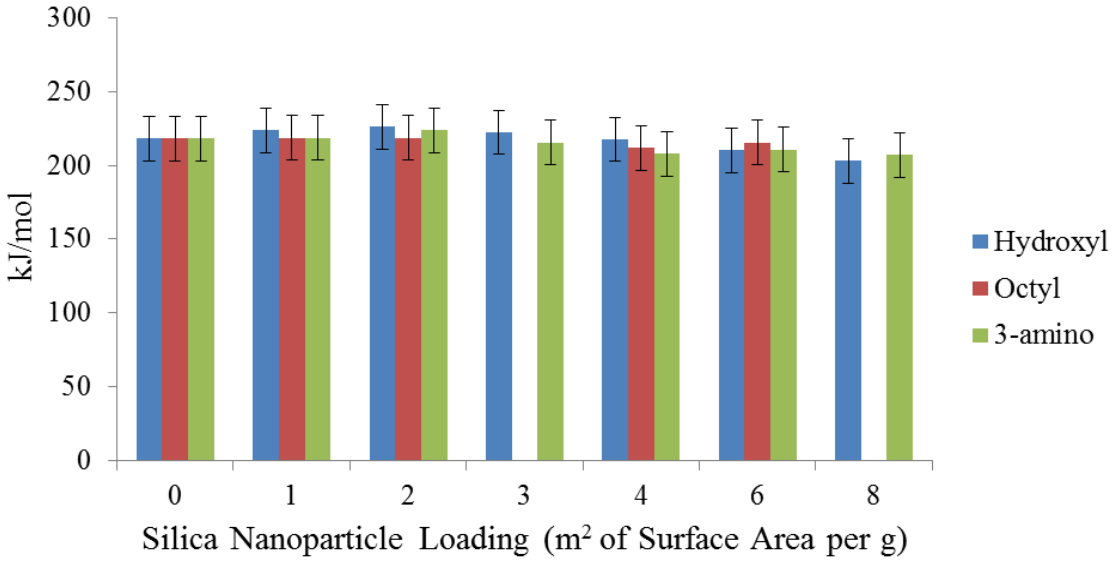

Figure 5. Integrated heats of reaction of each sample at different loading levels. Neither the type of surface modification nor the loading level has a significant influence on the total heat of reaction.

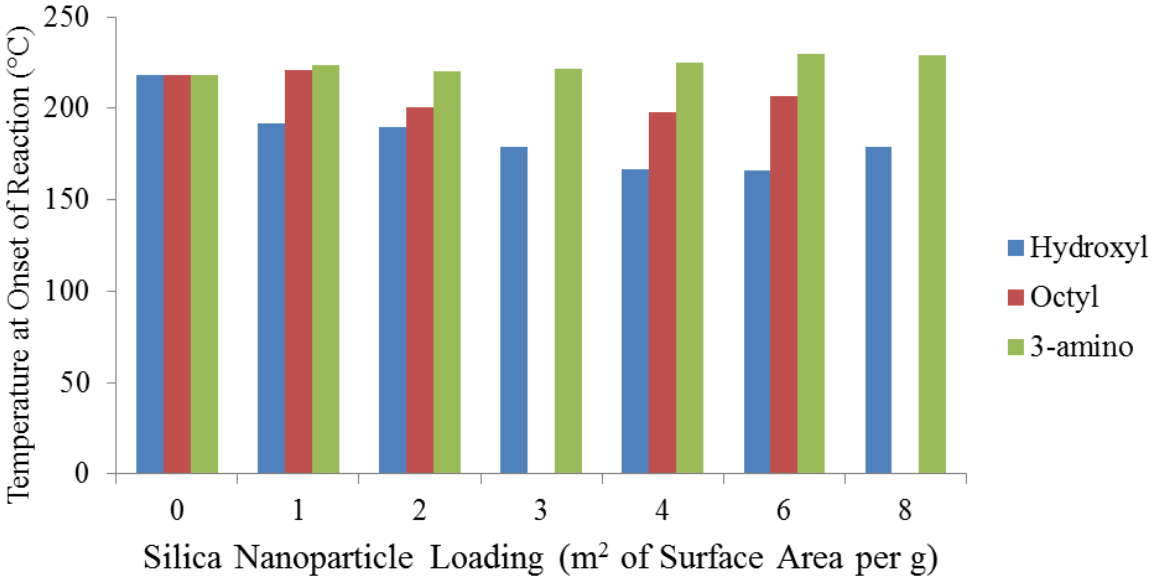

Figure 6. Reaction onset temperatures of each sample at different loading levels. Higher loadings of silica nanoparticles with hydroxyl moieties at the surface show a reduced onset temperature, indicating catalytic action.

3.4 The Influence of Surface Modification on Glass Transition Temperature

Figure 7 shows the T_g of postcured samples as measured by TMA. DSC measurement of postcured samples revealed no additional cure above the postcuring temperature of 290 °C which indicates that these samples had approached full conversion. This figure shows that nanocomposites with hydroxyl surfaces show an increased glass transition temperature with low particle loading levels but no further increase at higher loading levels. For octyl modified surfaces, higher loading levels are necessary to increase the glass transition temperature. Nanocomposites fabricated with 3-aminopropyl modified surfaces show no real increase in glass transition temperature. This may be a result of 'defects' in the network structure caused by the reaction of the surface amine moiety with cyanate ester monomer.

Figure 8 shows T_g of non-postcured samples as measured by TMA. DSC measurement showed different amounts of unreacted material for each of the samples. T_g is highly dependent on overall monomer conversion. Higher loadings of nanoparticles with hydroxyl surfaces show a higher glass transition temperature compared to lower loadings cured under the same conditions. This increase is likely due one of two things; increased conversion or reduced chain mobility caused by higher particle loading levels. As this trend is not observed in the other nanocomposite samples, the increase in glass transition temperature is likely a consequence of higher overall monomer conversion due to the catalytic action of the surface hydroxyl moieties rather than reduced chain mobility.

All non-postcured samples show lower glass transition temperatures than postcured samples. Additionally, there is not a significant difference in the fully-cured glass transition temperature of nanocomposites with hydroxyl and octyl functionalized nanoparticles while the chemically active 3-aminopropyl surface (which introduces defects into the network) has little effect on the glass transition temperature. This result indicates that the degree of overall conversion of cyanate ester groups to triazine ring crosslinks is more important than the interfacial interaction between the silica nanoparticle reinforcement and the cyanate ester matrix with regard to producing a high T_g nanocomposite.

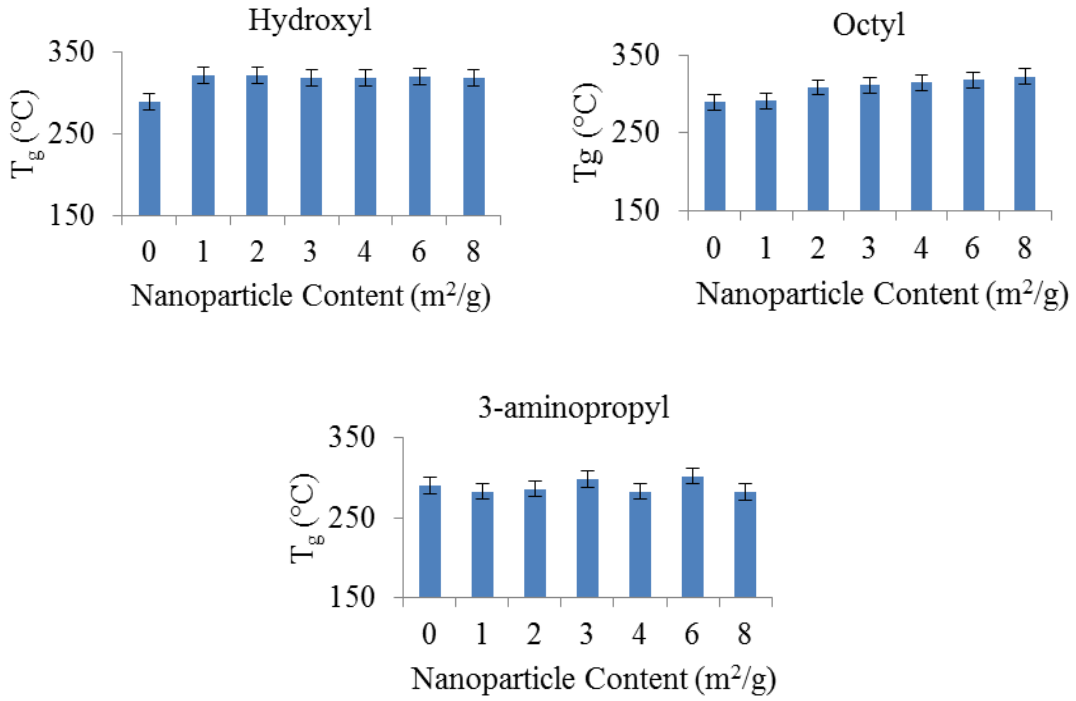

Figure 7. Glass transition temperature of postcured samples as measured by TMA.

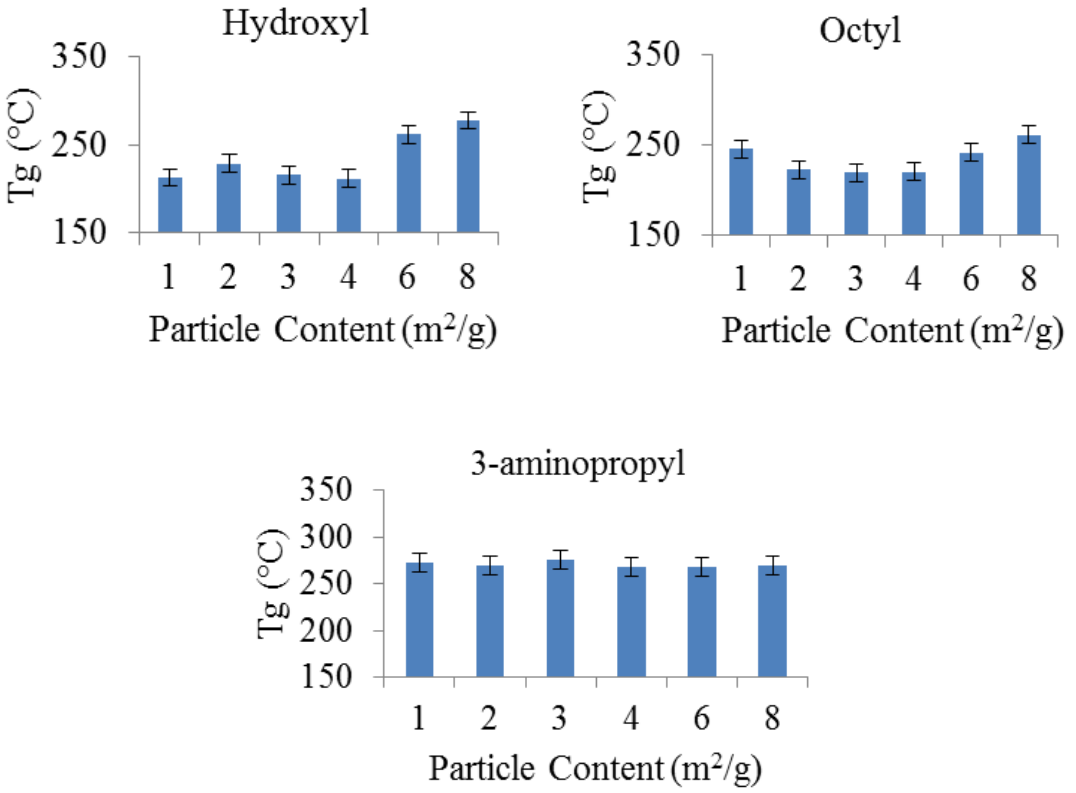

Figure 8. Glass transition temperature of non-postcured samples as measured by TMA.

4. CONCLUSIONS

A series of modified silica nanoparticle/cyanate ester nanocomposites have successfully been fabricated. AFM imaging revealed that the chemically active surface showed the best particle dispersion. Thermal analysis showed no apparent influence of the nanoparticle surface on the curing reaction pathway. Nanoparticles with hydroxyl surfaces showed an apparent catalytic effect that was not observed with other particles. This catalytic effect was found to increase the glass transition temperature of non-postcured samples. Overall monomer conversion was found to be a more important than nanoparticle surface chemistry with regard to producing a nanocomposite with a high glass transition temperature.

5. REFERENCES

1. Hussain, Farzana; Hojjati, Mehdi; Okamoto, Masami; Gorga, Russell. "Polymer-matrix Nanocomposites, Processing, Manufacturing, and Application: An Overview." Journal of Composite Materials. 40 (2006): 1511-1575.

2. Sangermano, M.; Malucelli, G.; Amerio, E.; Priola, A.; Billi, E.; Rizza, G. "Photopolymerization of Epoxy Coatings Containing Silica Nanoparticles." Process in Organic Coatings. 54 (2005): 134-138.

3. Mahrholz, T.; Stangle, J.; Sinapius, M. "Quantitation of the Reinforcement Effect of Silica Nanoparticles Used in Liquid Composite Moulding Processes." Composites Part A: Applied Science and Manufacturing. 40 (2009): 235-243.

4. Tang, J.; Lin, G.; Yang, H.; Jiang, G.; Chen-Yang, Y. "Polyimide-Silica Nanocomposites Exhibiting Low Thermal Expansion Coefficient and Water Absorption From Surface-Modified Silica." Journal of Applied Polymer Science. 104 (2007): 4096-4105.

5. Nelson, J.; MacCrone, R.; Schadler, L.; Reed, C.; Keefe, R. "Polymer Nanocomposite Dielectrics – The Role of the Interface". IEEE Transactions on Dielectrics and Electrical Insulation. 12 (2005): 629-643.

6. Mortezaei, Mehrzad; Famili, Mohammad; Kokabi, Mehrdad. "The Role of Interfacial Interactions on the Glass-Transition and Viscoelastic Properties of Silica/Polystyrene Nanocomposite." Composites Science and Technology. 71 (2011): 1039-1045.

7. Baller, Jorg; Becker, Nora; Ziehmer, Markus; Thomassey, Matthieu; Zielinski, Bartosz; Muller, Ulrich; Sanctuary, Roland. "Interactions Between Silica Nanocomposites and an Epoxy Resin Before and During Network Formation." Polymer. 50 (2009): 3211-3219.

8. Goertzen, W.; Kessler, M. "Dynamic Mechanical Analysis of Fumed Silica/Cyanate Ester Nanocomposites." Composites Part A: Applied Science and Manufacturing. 39 (2008): 761-768.

9. Taha, Elhussein; Wu, Jun-tao; Gao, Kai; Guo, Lin. “Preparation and Properties of Fumed Silica/Cyanate Ester Nanocomposites.” Chinese Journal of Polymer Science. 30 (2012): 530-536.

10. Goertzen, W.; Sheng, X.; Akinc, M.; Kessler, M. “Rheology and Curing Kinetics of Fumed Silica/Cyanate Ester Nanocomposites.” Polymer Engineering & Science. 48 (2008): 875-883.

11. Hammerton, Ian. Chemistry and Technology of Cyanate Ester Resins. Bury St. Edmunds: Blackie Academic & Professional, 1994.